Oct 17th, 12:00 AM

Design of Cold-formed Steel Stiffened Elements with Multiple Longitudinal Intermediate Stiffeners

Benjamin W. Schafer

Teoman Pekoz

Thirteenth International Specialty Conference on Cold-Formed Steel Structures
St. Louis, Missouri U.S.A., October 17-18, 1996

DESIGN OF COLD-FORMED STEEL STIFFENED ELEMENTS WITH MULTIPLE LONGITUDINAL INTERMEDIATE STIFFENERS

Benjamin Schafer[1] & Teoman Peköz[2]

ABSTRACT

Current specification procedures for calculating the bending strength of members with multiple longitudinal intermediate stiffeners in the compression flange have been found to be inadequate. A new procedure for calculating the effective width of stiffened elements with multiple intermediate stiffeners is presented. The new method introduces the calculation of a buckling coefficient for overall buckling of the entire stiffened element as a unit, and local buckling of the subelement plates between stiffeners. The expression for calculating overall buckling is derived and verified via comparison to numerical methods. The minimum buckling coefficient from the two modes (local and overall) is used to calculate the critical buckling stress for the element. Using Winter's equation the effective width of the element is determined. The effective width is distributed as two strips at the corners, in a manner similar to elements without intermediate stiffeners. The resulting section is found to be a reliable predictor of the bending strength of members with multiple intermediate stiffeners in the compression flange.

1 INTRODUCTION

The use of longitudinal stiffeners in the compression flange of cold-formed steel members is known to increase the ultimate strength of the member. Of course, the stiffeners also increase the complexity of the behavior. Due to the introduction of the stiffener, two modes of buckling (local and overall) occur in the element. Understanding which of these modes dominate, and thus how these modes can be used to predict the post-buckling capacity is required. It has been shown that current specification methods for the prediction of the strength of these sections are inadequate [Schafer and Peköz (1994)].

The methodology for this paper is to first examine the elastic buckling behavior, and then determine how to use that information for prediction of the ultimate strength. At all times,

[1]Graduate Research Assistant, Department of Civil and Environmental Engineering, Cornell University, Ithaca, New York
[2]Professor, Department of Civil and Environmental Engineering, Cornell University, Ithaca, New York

it was kept in mind that the final method should be a procedure which can be performed by hand, and thus appropriate for inclusion in a cold-formed steel design specification. To this end, a general solution for the elastic buckling is developed. The general solution is truncated and a simple method for determination of the elastic buckling stress is presented. Next, using effective width concepts analogous to that originally used by Winter (1946) a simple procedure is determined for calculating the ultimate strength. The proposed method is then compared to existing experimental and numerical data.

2 ELASTIC BUCKLING

In order to examine and understand the behavior of a plate/stiffener assembly the elastic buckling behavior must be known. Using the simplifying assumption that a stiffened element may be adequately modeled as a simply supported plate, a variety of methods for calculating the elastic buckling behavior exist. In Schafer and Peköz (1994) several methods are discussed and compared for approximating the elastic buckling stress of elements with multiple intermediate stiffeners. In Schafer (1995) different numerical methods for calculating elastic buckling behavior are investigated and compared. A classical method for calculating the elastic buckling behavior based on using a Fourier series for the deflected shape of the plate/stiffener assembly is fully developed here.

2.1 Solution by Fourier Series

The Fourier series solution is first developed in general form (arbitrary number of sine terms). A computer program is implemented for the solution using the general form. Then, the exact equations are derived and presented when only the first sine term is included. This, truncated Fourier series solution, is presented as a hand method for calculation of the buckling stress for overall buckling.

2.1.1 Derivation

The procedure for deriving the buckling stress begins by postulating a functional form for the deflected shape of the plate/stiffener assembly. The next step entails calculating the internal strain energy and external work of the system. This begins by determining the internal strain energy of the plate and the external work of the load on the plate. The internal strain energy and external work of the stiffeners comes next. With the energies known the potential energy can be formulated. The potential energy of the plate/stiffener assembly is equal to the sum of the internal strain energy minus the sum of the external work. By the Rayleigh-Ritz method it is known that the variation of the potential energy with respect to the displacement coefficients (i.e. the coefficients of the Fourier series) must be zero. This variation is completed, and leads to a infinite system of equations. By truncating the Fourier series we are left with a number of equations equal to the number of sine terms kept. The resulting system of equations provide a complete description of the elastic buckling behavior.

The details of the derivation for the problem shown in Figure 1 are presented below:

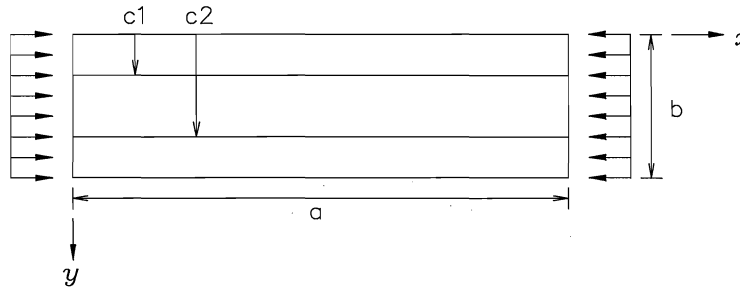

Figure 1 Schematic of SS Plate with Two Stiffeners in Pure Compression

As discussed the deflected shape is assumed to be in the form of a double Fourier series. The summation over m terms is in the longitudinal direction, and the summation over n terms is in the transverse direction.

$$w = \sum_m \sum_n a_{mn} \sin\left(\frac{m\pi x}{a}\right) \sin\left(\frac{n\pi y}{b}\right) \qquad \text{Eq 1}$$

The calculation of the internal strain energy of the plate is a well known result [Timoshenko and Gere (1936)] and is usually expressed as:

$$U_p = \frac{\pi^4 D}{2} \frac{ab}{4} \sum_m \sum_n a_{mn}^2 \left(\frac{m^2}{a^2} + \frac{n^2}{b^2}\right)^2 \qquad \text{Eq 2}$$

The external work of the uniform load on the plate can be shown to be:

$$W_p = \frac{\sigma t}{2} \frac{ab}{4} \sum_m \sum_n a_{mn}^2 \frac{m^2 \pi^2}{a^2} \qquad \text{Eq 3}$$

Now we turn to the internal strain energy of the stiffeners. Including only the bending energy, the strain energy of a given stiffener "i" is:

$$\begin{aligned} (U_s)_i &= \frac{1}{2} EI_i \int_0^a \left(\frac{\partial^2 w}{\partial x^2}\right)^2_{y=c_i} dx \\ &= \frac{\pi^4 EI_i}{4a^3} \sum_m m^4 \left(\sum_n a_{mn} \sin\left(\frac{n\pi c_i}{b}\right)\right)^2 \end{aligned} \qquad \text{Eq 4}$$

The external work of the uniform load on a given stiffener "*i*" is:

$$\begin{aligned}(W_s)_i &= \frac{1}{2}(P_s)_i \int_0^a \left(\frac{\partial w}{\partial x}\right)^2_{y=c_i} dx \\ &= \frac{1}{2}\sigma(A_s)_i \frac{\pi^2}{a^2}\frac{a}{2}\sum_m m^2 \left(\sum_n a_{mn}\sin\left(\frac{n\pi c_i}{b}\right)\right)^2\end{aligned} \qquad \text{Eq 5}$$

The total potential energy can then be expressed as:

$$\Pi = U_p - W_p + \sum_i (U_s)_i - \sum_i (W_s)_i \qquad \text{Eq 6}$$

The variation of the potential energy with respect to a_{mn} leads to a system of $m \times n$ linear equations. At this point several variable substitutions are made in order to express the equations in a simpler form:

$$\beta = \frac{a}{b} \quad k = \frac{\sigma b^2 t}{\pi^2 D} \quad \gamma_i = \frac{EI_i}{bD} \quad \delta_i = \frac{(A_s)_i}{bt} \quad \alpha_i = \frac{c_i}{b} \qquad \text{Eq 7}$$

With these substitutions the system of equations can be expressed as:

$$a_{mn}\left[\left(m^2 + n^2\beta^2\right)^2 - k\beta^2\right] + \sum_i \left(2\gamma_i - 2k\beta^2\delta_i m^2\right)\sin(n\pi\alpha_i)\sum_p a_{mp}\sin(p\pi\alpha_i) = 0 \qquad \text{Eq 8}$$

for only one longitudinal sine term, namely $m = 1$, the expression simplifies to:

$$a_{1n}\left[\left(1 + n^2\beta^2\right)^2 - k\beta^2\right] + \sum_i \left(2\gamma_i - 2k\beta^2\delta_i\right)\sin(n\pi\alpha_i)\sum_p a_{1p}\sin(p\pi\alpha_i) = 0 \qquad \text{Eq 9}$$

this leads to a system of equations which may be placed in the form $[K]_{n\times n}\{a\}_{n\times 1} = 0$, where n is the number of transverse sine terms included. For nonzero $\{a\}$ the condition $\det[K] = 0$ must be true. Using this condition one can find the solution for k, given β.

2.1.2 Truncated Fourier Series Solution

In the previous section the elastic buckling solution is presented for an arbitrary number of transverse sine terms (Equation 9). For plate/stiffener assemblies loaded in pure compression one sine wave in the transverse direction may provide an adequate description of the deflected shape for the overall buckling of the plate. Figure 2 shows an example where using only the first sine term to represent the overall buckling of the plate/stiffener assembly is adequate.

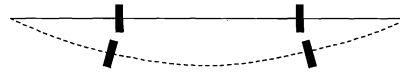

Figure 2 Displaced Shape of Plate with Multiple Stiffeners (Overall Buckling)

If only the first transverse term is kept, namely $n = 1$, then the solution to Equation 9 of the previous section is simplified. In this case, k may be solved for directly.

$$k = \frac{\left(1+\beta^2\right)^2 + 2\sum_i \gamma_i \sin^2(\pi\alpha_i)}{\beta^2\left(1+2\sum_i \delta_i \sin^2(\pi\alpha_i)\right)} \qquad \text{Eq 10}$$

In addition, by taking the derivative with respect to β, one can show that the critical β_{cr} (the β when k is a minimum) is:

$$\beta_{cr} = \left(2\sum_i \gamma_i \sin^2(\pi\alpha_i)+1\right)^{1/4} \qquad \text{Eq 11}$$

Using this result, the critical buckling coefficient (minimum k) is found to be:

$$k_{cr} = \frac{\left(1+\beta_{cr}^2\right)^2 + 2\sum_i \gamma_i \sin^2(\pi\alpha_i)}{\beta_{cr}^2\left(1+2\sum_i \delta_i \sin^2(\pi\alpha_i)\right)} \qquad \text{Eq 12}$$

Since the solution is for only one transverse sine term, the deflected shape is an approximation of the overall buckling of the plate stiffener assembly (as shown in Figure 2). This mode of buckling, described here as overall buckling of the element, is also called stiffener buckling, or distortional buckling, in the literature. Regardless of the terminology, the characteristic shape of the buckling mode is the same.

2.2 Examination of Truncated Fourier Series Solution

Using a computer program written in MATLAB the solution to Equation 8 is found for an arbitrary number of sine terms in the longitudinal or transverse direction. The longitudinal sine terms do not interact. Therefore, only the first longitudinal term is required and Equation 9 can be used to investigate the transverse sine terms. This section begins with an investigation of how many transverse sine terms are needed before the solution satisfactorily converges. Next, calculation of the local buckling stress is considered. Finally, a truncation of the Fourier series using only the first term (Eq 10) is compared to the finite strip solution.

2.2.1 Influence of the Number of Transverse Sine Terms

In order to examine the influence of the number of included transverse terms, Equation 9 is solved for three sets of examples. *Example 1* consists of a plate with 3 evenly spaced stiffeners, at four different stiffener sizes. *Example 2* consists of a plate with 2 stiffeners with location symmetrical about the centerline, and four different plate subelement widths. *Example 3* consists of a plate with 4, 6, 8, or 10 evenly spaced stiffeners.

In addition, Equations 11 and 12 are also used directly to calculate the critical plate buckling coefficient by hand. Table 1 summarizes the results of the analysis, "Numerical"

refers to the computer solution, "Hand" refers to the first term Fourier series solution (Eq 11 and 12). K_{cr} in Table 1 is defined as the minimum plate buckling coefficient.

Table 1 Results for Study of Needed Number of Transverse Terms

number of	*location*			*Numerical*		*Hand*
stiffeners	αi	δi	γi	*# terms*	*Kcr*	*Kcr*
3	*evenly*	0.05	5	1	9.32	9.30
-	*spaced*	-	-	3	9.32	
-	-	-	-	6	9.32	
-	-	-	25	1	18.42	18.42
-	-	-	-	6	18.42	
-	-	-	50	1	25.30	25.30
-	-	-	-	6	25.30	
-	-	-	100	1	35.88	35.04
-	-	-	-	6	35.88	
2	0.1,0.9	0.05	25	1	8.34	8.34
-	-	-	-	6	8.10	
-	0.2,0.8	-	-	1	13.03	13.02
-	-	-	-	6	12.90	
-	0.3,0.7	-	-	1	16.20	16.18
-	-	-	-	6	16.18	
-	0.4,0.6	-	-	1	17.92	17.89
-	-	-	-	6	17.90	
4	*evenly*	0.025	10	1	14.49	14.47
-	*spaced*	-	-	6	14.49	
6	-	-	-	1	16.07	16.04
-	-	-	-	6	16.07	
8	-	-	-	1	17.23	17.21
-	-	-	-	6	17.23	
10	-	-	-	1	18.10	18.09
-	-	-	-	6	18.10	

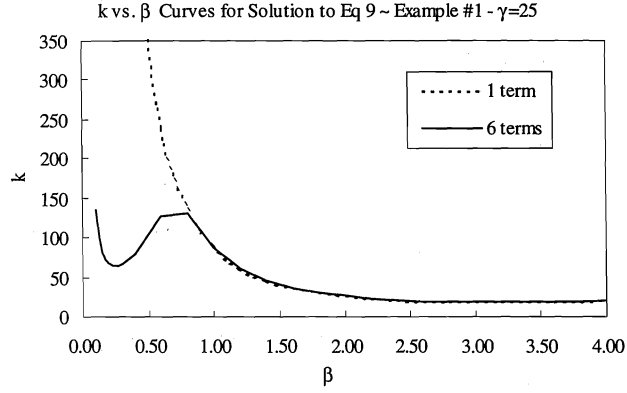

Figure 3 Typical Aspect Ratio vs. Buckling Coefficient Curves

Comparing the hand and numerical solutions in Table 1 it is concluded that for the problems studied only one transverse sine term is needed to capture the critical plate buckling coefficient. Inherent in this conclusion, is the assumption that the critical buckling

mode is analogous to that shown in Figure 2. This should be the case for any reasonable stiffener arrangement. An investigation of the entire picture (rather than just the minimum) reveals the role of local buckling. Figure 3 shows the complete results for Example 1 (3 stiffeners), when $\gamma = 25$. It is clear from the figure that the first sine term does not account for the local buckling. However, in all the cases studied overall buckling governed the behavior.

2.2.2 Local Buckling and Overall Buckling

Overall buckling is distinct from local buckling, which is defined as the buckling of the plate subelements. A plate subelement is defined as the flat plate between stiffeners or the supported edge (Figure 4).

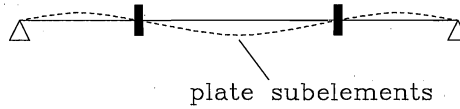

Figure 4 Plate Subelements control Local Buckling

The local buckling mode is sometimes of interest for plates with multiple stiffeners. Local buckling characteristics can be accurately approximated by assuming that the subelement is simply supported. Therefore, a plate buckling coefficient of 4 is employed for calculation of the local buckling stress of the plate subelement. The critical buckling length for local buckling in pure compression is equal to the subelement width. For a subelement plate of width b_i, and overall plate width of b_o, the local buckling coefficient is:

$$k_l = 4\left(\frac{b_o}{b_i}\right)^2 \qquad \text{Eq 13}$$

2.2.3 Comparison to Finite Strip Solution

Accurate numerical methods exist that give the elastic buckling characteristics of members with arbitrary geometry. One such procedure called "finite strip" is implemented in the program BFINST. An excellent summary of the method is presented in Hancock (1994). In order to study the accuracy of the presented solution method, six example problems are compared using BFINST, and the first term of the Fourier series solution.

The example problems are based on the geometry of the compression flange of hat shaped members analyzed in Schafer and Peköz (1994). The stiffeners are modeled as a v-shaped groove. The moment of inertia of the stiffeners about their own axis is selected to be equal to the minimum moment of inertia specified in the AISI Specification [AISI (1991)]. Table 2 summarizes the overall geometry of the example problems and presents the results for the three methods. The theory developed for the Fourier series solution assumes that the stiffeners are symmetrical about the axis of the plate. For the example problem the stiffeners are on one side of the plate. For calculating γ, the moment of inertia of these one-sided stiffeners is taken about the axis of the plate.

Table 2 Comparison of Solution Method with Finite Strip

number of stiffeners	*b/t of plate subelement*	*Kcr*		*βcr*	
		BFINST	*first term Fourier*	*BFINST*	*first term Fourier*
2	30	17.4	15.3	3.2	3.3
2	50	19.6	17.4	3.2	3.4
3	30	16.7	15.3	3.0	3.3
3	50	18.9	17.3	3.2	3.3
4	30	16.3	15.2	3.1	3.2
4	50	18.7	17.3	3.1	3.3

In the example problems studied overall buckling governed the behavior. The first term approximation of the Fourier series gives a reasonable approximation of both, k_{cr}, the minimum plate buckling coefficient and, β_{cr}, the critical buckling aspect ratio.

2.3 Proposed Method for Elastic Buckling Calculations

Based on the examples it is concluded that the first term approximation of the Fourier series solution is adequate for calculating the overall buckling characteristics. Local buckling can be approximated assuming simple supports for the plate subelements. The resulting expressions for the elastic buckling characteristics are therefore:

Local Buckling:

$$(\beta_{cr})_{local} = \frac{b_i}{b_o} \qquad \text{Eq 14}$$

$$(k_{cr})_{local} = 4\left(\frac{b_o}{b_i}\right)^2 \qquad \text{Eq 15}$$

Overall Buckling:

$$(\beta_{cr})_{overall} = \left(2\sum_i \gamma_i \sin^2(\pi\alpha_i)+1\right)^{1/4} \qquad \text{Eq 16}$$

$$(k_{cr})_{overall} = \frac{\left(1+\beta_{cr}^2\right)^2 + 2\sum_i \gamma_i \sin^2(\pi\alpha_i)}{\beta_{cr}^2\left(1+2\sum_i \delta_i \sin^2(\pi\alpha_i)\right)} \qquad \text{Eq 17}$$

3 ULTIMATE STRENGTH

The equations developed give solutions only for elastic buckling. Post-buckling strength exists in the sections considered. Unfortunately, analytical solutions for the ultimate strength are cumbersome, because the problem involves consideration of large deflections

and nonlinear material behavior. In order to account for the post-buckling strength, the element is examined using a simple effective width procedure.

3.1 Effective Width

The effective width concept is used to provide a methodology for the design of members in the post-buckling range. For a stiffened element under uniform compression a nonlinear longitudinal stress develops across the element. The nonlinear longitudinal stress diagram is replaced by a uniform stress over two strips at the edges, each of width $b_{eff}/2$. Empirical formulas have been derived for finding the width of the strips, i.e. b_{eff}. Von Kármán (1932) is generally attributed with the first attempt for calculating the effective width. A correction to that original formula that is used extensively throughout the world is attributed to Winter (1946).

3.1.1 Local Buckling Based Effective Width

For members with multiple longitudinal intermediate stiffeners it may seem natural, in predicting the capacity, to assume the stiffeners break up the member in to many smaller stiffened elements (plate subelements). This assumes that the local buckling of the member (i.e. Figure 4) governs the behavior. For instance Figure 5 shows the effective strips for local buckling only, and a postulated nonlinear stress diagram based on this assumption.

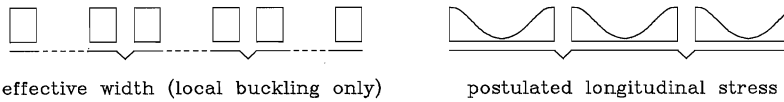

Figure 5 Postulated Local Buckling Based Effective Width

Use of a simple approach such as shown in Figure 5 yields highly unconservative strength prediction in almost all cases [Schafer and Peköz (1994)]. The authors are unaware of an example from numerical analysis or experimental work with multiple longitudinal intermediate stiffeners that exhibits a stress distribution fully dominated by local buckling as suggested in Figure 5. As a result of the failure of this approach a variety of methods for determining the ultimate strength of these elements has emerged. A thorough discussion of several different procedures including: Eurocode, Canadian Specification, AISI Specification, Column Buckling Model, Average Stress Procedure, Equivalent Effective Width Method, and Modified Kwon and Hancock can be found in Schafer and Peköz (1994). The procedure presented in this paper is an alternative to those methods.

3.1.2 Including Overall Buckling - Effective Width

For all cases with multiple stiffeners: including the numerical examples in this paper, the experimental work of König (1978), Papazian et al. (1994), and the numerical analysis of Schafer (1994), some 62 different geometry's in all, *the elastic overall buckling stress is lower than the local buckling stress.*. From finite element analysis it is found that when both overall buckling and local buckling exist, the longitudinal membrane stress distribution at failure is similar to the distributions shown in Figure 6.

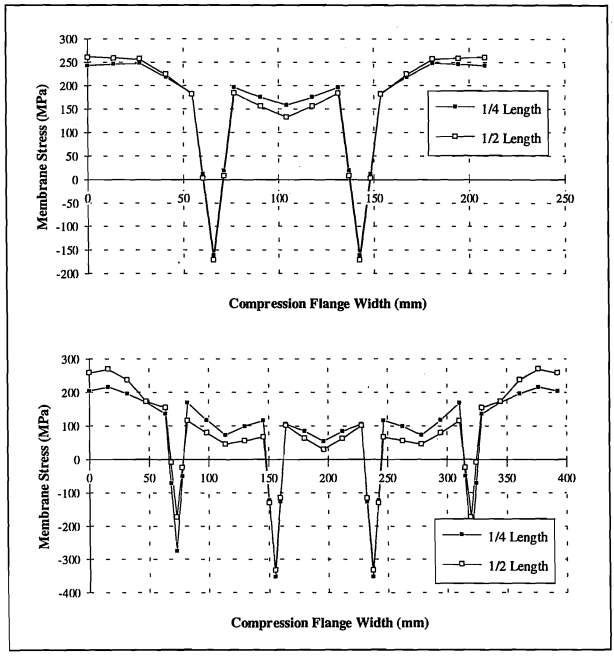

Figure 6 Longitudinal Stress Profiles from Finite Element Analysis [Schafer and Peköz (1994)]

The shape, or overall trend in the stress distribution for the overall buckling mode is similar to that of one for a stiffened element without intermediate stiffeners (i.e. the classical effective width solution). Analysis shows that the maximum compressive stresses are typically carried at the edges, as shown in Figure 6. Therefore, it is postulated by the authors that for all elements with multiple stiffeners it is conservative and reasonable to assume effective portions on the edges only, rather than separate reductions in the plate subelements. As such, it is proposed that two strips of width $b_{eff}/2$ at the edges be considered as the effective width. The suggested effective width procedure is shown schematically in Figure 7.

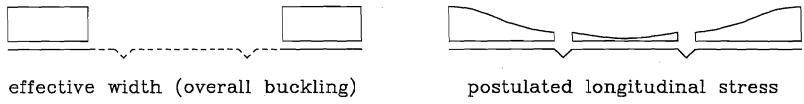

Figure 7 Postulated Distortional Buckling Based Effective Width

It was found that the stiffeners can be approximated as if they are bending about the plane of the plate (Table 2). As a result, it is assumed that the effective strips are distributed at the centerline of the plate. Since overall buckling describes the behavior of the entire element, the reduction from the effective width formula is applied over the entire element. For simplicity, the effective portion can be assumed as a flat plate at the centerline of the actual plate.

3.2 Formula for Determining Effective Width

The effective width of an element can be presented in terms of the average failure stress across the element (f_u). In these terms one can readily examine several different expressions for the effective width on the same plot (see Figure 8). The curves show the form of several different models: elastic, Winter [Winter (1946)], Modified Winter [Kwon and Hancock (1992)], Von Kármán [Von Kármán (1932)] and Johnston Parabola [Johnston (1976)].

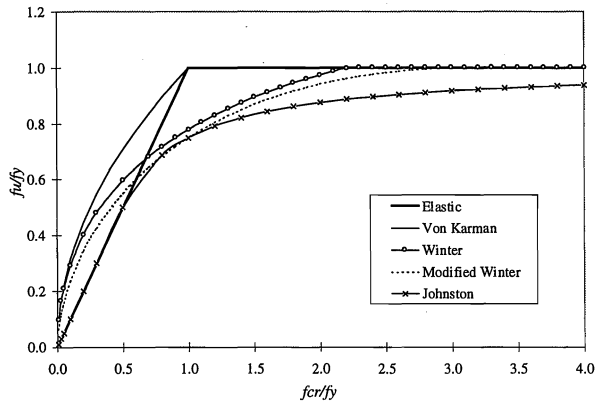

Figure 8 Possible Effective Width Curves

Von Kármán's curve represents the first attempt to directly account for the nonlinear longitudinal stress distribution. It has been found to be inadequate, due to the residual stresses and imperfections which exist in actual plates. Winter's formula is an empirical correction to Von Kármán's procedure. Winter showed his formula to adequately represent the strength of stiffened and unstiffened elements undergoing local buckling. The Modified Winter curve is a further correction proposed by Kwon and Hancock. The Modified Winter curve attempts to account for the slightly different behavior observed in edge stiffened members undergoing distortional buckling. Johnston's Parabola is a conservative approximation and in general is a safe lower bound. The elastic curve fails to capture the actual behavior. Using elastic buckling directly can lead to either conservative or unconservative design depending on the ratio of f_{cr}/f_y.

It has already been mentioned that the overall buckling mode, postulated as the typical failure mode, is analogous to local buckling of a stiffened element without intermediate stiffeners. Therefore, the well established Winter formula is selected as a possibility for the effective width calculation. Although the distortional buckling mode which the Modified Winter curve is designed to account for is slightly different than the overall buckling mode expected here, they do share similarities. Both an edge stiffened element undergoing distortional buckling, and a stiffened element with intermediate stiffeners undergoing overall buckling, have a shorter wavelength local buckling mode present, that may cause a slight reduction in the post-buckling range, as reflected in the Modified Winter curve. Therefore, the Modified Winter curve is also selected for further study.

3.3 Proposed Method for Ultimate Strength

The first step is to calculate the plate buckling coefficient for the two modes. With the $(k_{cr})_{local}$ and $(k_{cr})_{overall}$ known, the smaller of the two is selected for use in determining the critical buckling stress. The critical buckling stress and the uniform compressive stress (f_1) acting on the element are used to calculate the reduction factor (χ). The reduction factor is then used to distribute an effective portion of the entire area to two strips at the edges of the plate. This is done by multiplying the reduction factor (χ) times the gross area of the stiffened element (A_g) divided by the plate thickness. Since the role of the stiffeners is to provide stability to the compression flange, the effective width is limited to the full flat plate width (b_o). The strips are placed at the centerline of the plate with width $b_{eff}/2$ and thickness equal to the plate thickness. The method is summarized in the following equations:

Effective Width Determination

$$b_{eff} = \chi\left(\frac{A_g}{t}\right) \le b_o \qquad \text{Eq 18}$$

$$\text{with: } \chi = \left(\frac{f_{cr}}{f_1}\right)^{0.5}\left(1-0.22\left(\frac{f_{cr}}{f_1}\right)^{0.5}\right) \quad \text{(Winter)} \qquad \text{Eq 19}$$

$$\text{or, } \chi = \left(\frac{f_{cr}}{f_1}\right)^{0.6}\left(1-0.25\left(\frac{f_{cr}}{f_1}\right)^{0.6}\right) \quad \text{(Modified Winter)} \qquad \text{Eq 20}$$

$$\text{where: } f_{cr} = k\frac{\pi^2 D}{b_o^2 t} \quad \text{and } k = \min\left((k_{cr})_{local}, (k_{cr})_{overall}\right) \qquad \text{Eq 21}$$

4 EVALUATION OF PROPOSED METHOD

In order to evaluate the proposed method, experimental results [König (1978)], [Papazian (1994)] and finite element analysis [Schafer (1995a)] have been gathered for comparison. In all cases the bending moments are recorded in *Nm*. In all cases the critical buckling stresses are calculated using Equations 14-17. The three methods compared are the AISI Specification and two variations of the proposed method. The first variation of the proposed method uses Winter's equation (Eq 19) for calculating the effective width. The second variation uses the Modified Winter equation (Eq 20).

4.1 Experiments by Papazian, Schuster, and Sommerstein

The results for the test to predicted ratios and buckling stresses are presented in Table 3. Members 9. .18 are for 2 stiffeners, 14. .26 are for 3, and 16. .24 for 4 stiffeners. Table 3 indicates that of the proposed methods, Winter's expression is less conservative than the Modified Winter. This conservatism is particularly important for the members with small overall buckling stresses, i.e., the four stiffener members.

4.2 Experiments by König

All of König's tests shown in Table 4 are for members with two stiffeners. The B series members may not be indicative of common practice. The B series has an overall *w/t* of 460 and the ratio of f_{cr}/f_y is approximately 0.05. For small ratios of f_{cr}/f_y the difference between Winter's expression and the Modified Winter expression can be large (see Figure 7). If the B series members are ignored Winter's test to predicted average is 1.03 and Modified Winter is 1.11 for the test to predicted ratios.

4.3 Numerical (Finite Element) Results by Schafer

The results for the 64 numerical analysis are summarized in Table 5 Summary Statistics of Test to Predicted Ratios for . The details of the results are in Table 6 and Table 7. The Winter expression yields excellent results for the 64 members analyzed.

4.4 Summary of Comparison

The experimental data covering 30 experiments and 64 numerical analysis for hat sections with two to four intermediate longitudinal stiffeners in the compression flange show the proposed methods to be markedly better than the current AISI Specification. Figure 9 Average Test to Predicted Ratio Results dramatizes this fact. It shows that the AISI Specification averages nearly 20% on the unconservative side for the 94 members. Winter's curve is proposed as the expression for determining the effective width.

Figure 9 Average Test to Predicted Ratio Results

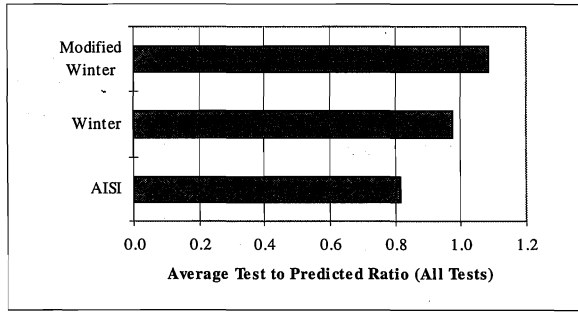

5 CONCLUSIONS

A method for the calculation of the ultimate strength of a stiffened element with multiple longitudinal intermediate stiffeners is proposed and validated. A simple solution (Eq 14-17) is derived and validated for calculating the elastic buckling stress of these elements. The method yields the critical buckling stress for the two buckling modes (local and overall) of the element. Examination of existing experimental and numerical data reveal that the overall buckling mode dominates the behavior. In fact, for all geometry's studied (62 different configurations) the overall buckling stress occurred at a lower value than the local buckling stress. Consistent with this observation, a simple effective width consisting of two strips at the corners is proposed. Winter's equation and a slight modification are compared for determination of the effective width. With the effective width known the

ultimate strength can be readily calculated. Comparison to existing data shows that either formulation (Winter or modified Winter) works better than existing procedures, and the original Winter's equation appears to give the best results.

REFERENCES

American Iron and Steel Institute (1991). "Load and Resistance Factor Design (LRFD) Cold-Formed Steel Design Manual." *American Iron and Steel Institute.*

Canadian Standards Association (1991). "CAN/CSA-S136-M89, Cold Formed Steel Structural Members." *Canadian Standards Association.*

Eurocode 3 Design of Steel Structures (1992). Part 1.3 Cold Formed Thin Gauge Members and Sheetings.

Johnston, B.G. (1976). **Guide to Stability Design Criteria for Metal Structures**, 3rd Ed., John Wiley and Sons, New York.

König, J. (1978). "Transversally Loaded Thin-Walled C-Shaped Panels With Intermediate Stiffeners." *Swedish Council for Building Research.*

Kwon, Y.B., Hancock, G.J. (1992). "Strength Tests of Cold-formed Channel Sections Undergoing Local and Distortional Buckling" *ASCE J. of Structural Engineering*, 117(2).

Papazian, R.P., Schuster, R.M., and Sommerstein, M. (1994). "Multiple Stiffened Deck Profiles." *Twelfth International Specialty Conference on Cold-Formed Steel Structures.*

Schafer, B.W., Peköz, T. (1994). "Behavior and Design of Cold-Formed Steel Compression Elements with Intermediate Stiffeners." *Structural Engineering Report,* School of Civil and Environmental Engineering, Cornell University

Schafer, B.W., (1995)."Progress Report No. 3: Behavior and Design of Flanges and Webs With Longitudinal Intermediate Stiffeners." *AISI Progress Report.*

Von Kármán, T., Sechler, E.E., Donnell, L.H. (1932). "The Strength of Thin Plates In Compression." *Transactions, ASME.*, Vol. 54, p.53

Winter, G. (1946). "Strength of Thin Steel Compression Flanges." *ASCE, Paper No. 2305*, Trans., Vol. 112, p.1.

Table 3 Test to Predicted Ratios & Buckling Stress for Papazian, Schuster and Sommerstein Experiments

	Observed		*Mtest*		*Mtest*	*Modified*	*Mtest*	*critical stress (MPa)*	
Member	*Moment*	*AISI*	*M aisi*	*Winter*	*M winter*	*Winter*	*M m.winter*	*overall*	*local*
9	1082	1609	0.67	1095	0.99	1045	1.04	215	435
10	1063	1611	0.66	1097	0.97	1047	1.02	215	426
11	1627	1680	0.97	1688	0.96	1659	0.98	197	448
12	1752	1633	1.07	1646	1.06	1633	1.07	194	452
13	3666	4113	0.89	3944	0.93	3722	0.98	175	556
18	3701	4117	0.90	3949	0.94	3726	0.99	175	546
14	1076	1601	0.67	1165	0.92	1070	1.01	110	368
15	1076	1602	0.67	1165	0.92	1069	1.01	108	361
19	1563	1602	0.98	1633	0.96	1612	0.97	108	435
20	1589	1620	0.98	1651	0.96	1630	0.97	109	448
25	3628	4136	0.88	4133	0.88	3744	0.97	93	529
26	3678	4090	0.90	4093	0.90	3707	0.99	92	524
16	1014	1648	0.62	1199	0.85	1054	0.96	56	292
17	1013	1648	0.61	1199	0.84	1054	0.96	56	292
21	1664	1623	1.03	1665	1.00	1634	1.02	67	419
22	1677	1561	1.07	1610	1.04	1580	1.06	67	419
23	3636	4118	0.88	4242	0.86	3717	0.98	58	508
24	3462	4096	0.85	4220	0.82	3715	0.93	58	508
		Average	**0.85**		**0.93**		**1.00**		
		Std. Dev.	**0.16**		**0.07**		**0.04**		

Table 4 Test to Predicted Ratios and Buckling Stresses for König's Experiments

	Observed		*Mtest*		*Mtest*	*Modified*	*Mtest*	*critical stress (MPa)*	
Member	*Moment*	*AISI*	*M aisi*	*Winter*	*M winter*	*Winter*	*M m.winter*	*overall*	*local*
A42	12460	16738	0.74	11770	1.06	10780	1.16	102	284
A51	13180	16728	0.79	12450	1.06	11530	1.14	127	309
A52	13270	17561	0.76	13060	1.02	12090	1.10	130	319
A61	14350	17588	0.82	14130	1.02	13220	1.09	161	367
A62	13270	16847	0.79	13430	0.99	12540	1.06	152	340
B41	994	716	1.39	1259	0.79	1003	0.99	17	34
B42	1054	741	1.42	1287	0.82	1024	1.03	16	35
B51	1054	1470	0.72	1465	0.72	1182	0.89	23	37
B52	1114	1540	0.72	1506	0.74	1211	0.92	22	37
B61	1144	1621	0.71	1651	0.69	1347	0.85	27	40
B62	1144	1626	0.70	1677	0.68	1378	0.83	29	41
B71	1174	1605	0.73	1762	0.67	1483	0.79	35	42
		Average	**0.86**		**0.85**		**0.99**		
		Std. Dev.	**0.26**		**0.16**		**0.13**		

Table 5 Summary Statistics of Test to Predicted Ratios for Schafer and Peköz Analysis

FEM to Predicted	*AISI*		*Winter*		*Modified Winter*	
Ratios for...	Average	Std. Dev.	Average	Std. Dev.	Average	Std. Dev.
All Data	**0.80**	0.11	**1.01**	0.08	**1.13**	0.08
Web=100mm	**0.84**	0.11	**1.06**	0.07	**1.18**	0.07
Web=50mm	**0.77**	0.11	**0.95**	0.05	**1.08**	0.04
2 Stiffeners	**0.76**	0.13	**1.03**	0.06	**1.12**	0.06
3 Stiffeners	**0.81**	0.08	**1.01**	0.09	**1.14**	0.08
4 Stiffeners	**0.84**	0.10	**0.98**	0.10	**1.14**	0.09

Table 6 Test to Predicted Ratios and Buckling Stresses for Schafer and Peköz ~ Web=100mm

Member	FEM	AISI	$\frac{M_{fem}}{M_{aisi}}$	Winter	$\frac{M_{fem}}{M_{winter}}$	Modified Winter	$\frac{M_{fem}}{M_{m.winter}}$	critical stress (MPa) overall	local
n2-wt20-I2	3553	3604	0.99	3459	1.03	3367	1.06	356	1835
n2-wt30-I2	3969	4603	0.86	3725	1.07	3546	1.12	208	815
n2-wt35-I2	4180	5367	0.78	3846	1.09	3624	1.15	173	599
n2-wt50-I2	4442	5917	0.75	3866	1.15	3505	1.27	90	294
n2-wt70-I2	4242	5956	0.71	4097	1.04	3599	1.18	58	150
n2-wt20-I1	3350	3464	0.97	3173	1.06	3084	1.09	329	1835
n2-wt30-I1	3684	4434	0.83	3440	1.07	3269	1.13	194	815
n2-wt35-I1	3776	5110	0.74	3480	1.09	3261	1.16	149	599
n2-wt45-I1	3991	5473	0.73	3634	1.10	3334	1.20	106	362
n2-wt50-I1	4184	5599	0.75	3708	1.13	3371	1.24	92	294
n2-wt70-I1	4032	5662	0.71	3871	1.04	3399	1.19	55	150
n2-wt20-I0.5	3303	3324	0.99	2869	1.15	2776	1.19	274	1835
n2-wt30-I0.5	3460	4084	0.85	3161	1.09	2991	1.16	171	815
n2-wt35-I0.5	3470	4855	0.71	3242	1.07	3030	1.15	137	599
n2-wt50-I0.5	3283	5356	0.61	3224	1.02	2891	1.14	67	294
n2-wt70-I0.5	3341	5433	0.61	3403	0.98	2952	1.13	42	150
n3-wt20-I2	3933	4619	0.85	3680	1.07	3481	1.13	183	1835
n3-wt30-I2	4431	5568	0.80	3928	1.13	3605	1.23	110	815
n3-wt35-I2	4542	4673	0.97	4012	1.13	3633	1.25	90	599
n3-wt50-I2	4633	4711	0.98	4191	1.11	3667	1.26	55	294
n3-wt70-I2	4164	4598	0.91	4341	0.96	3663	1.14	34	150
n3-wt20-I1	3590	4385	0.82	3368	1.07	3184	1.13	173	1835
n3-wt30-I1	3940	5045	0.78	3581	1.10	3278	1.20	101	815
n3-wt35-I1	4125	4683	0.88	3653	1.13	3298	1.25	81	599
n3-wt45-I1	4208	4645	0.91	3759	1.12	3311	1.27	57	362
n3-wt50-I1	4183	4651	0.90	3801	1.10	3312	1.26	49	294
n3-wt70-I1	3941	4555	0.87	3924	1.00	3295	1.20	29	150
n3-wt20-I0.5	3619	3982	0.91	3103	1.17	2928	1.24	161	1835
n3-wt30-I0.5	3435	4490	0.77	3284	1.05	2997	1.15	91	815
n3-wt35-I0.5	3384	4629	0.73	3342	1.01	3007	1.13	72	599
n3-wt50-I0.5	3534	4592	0.77	3467	1.02	3006	1.18	42	294
n3-wt70-I0.5	3118	4512	0.69	3565	0.87	2978	1.05	24	150
n4-wt20-I2	4069	5258	0.77	3808	1.07	3499	1.16	111	1835
n4-wt30-I2	4568	5971	0.77	4035	1.13	3584	1.27	68	815
n4-wt35-I2	4569	4262	1.07	4110	1.11	3600	1.27	55	599
n4-wt50-I2	4526	4277	1.06	4272	1.06	3610	1.25	34	294
n4-wt70-I2	3799	4125	0.92	4407	0.86	3588	1.06	21	150
n4-wt20-I1	3663	4266	0.86	3477	1.05	3195	1.15	106	1835
n4-wt30-I1	4167	4695	0.89	3669	1.14	3255	1.28	62	815
n4-wt35-I1	4194	4254	0.99	3733	1.12	3264	1.28	50	599
n4-wt50-I1	4109	4287	0.96	3866	1.06	3258	1.26	30	294
n4-wt70-I1	3659	4152	0.88	3976	0.92	3226	1.13	18	150
n4-wt20-I0.5	3398	4266	0.80	3194	1.06	2933	1.16	99	1835
n4-wt30-I0.5	3613	4695	0.77	3356	1.08	2972	1.22	56	815
n4-wt35-I0.5	3704	4229	0.88	3408	1.09	2971	1.25	45	599
n4-wt50-I0.5	3388	4274	0.79	3519	0.96	2955	1.15	26	294
n4-wt70-I0.5	3051	4150	0.74	3605	0.85	2917	1.05	15	150

Table 7 Test to Predicted Ratios and Buckling Stresses for Schafer and Peköz ~Web=50mm

Member	FEM	AISI	$\frac{M_{fem}}{M_{aisi}}$	Winter	$\frac{M_{fem}}{M_{winter}}$	Modified Winter	$\frac{M_{fem}}{M_{m.winter}}$	critical stress (MPa) overall	local
L-n2-wt30-I2	1713	2069	0.83	1747	0.98	1665	1.03	208	815
L-n2-wt40-I2	1768	2516	0.70	1837	0.96	1715	1.03	143	459
L-n2-wt50-I2	1763	2645	0.67	1812	0.97	1646	1.07	90	294
L-n2-wt60-I2	1755	2736	0.64	1961	0.89	1767	0.99	82	204
L-n2-wt70-I2	1804	2570	0.70	1917	0.94	1689	1.07	58	150
L-n2-wt10-I1	1264	1076	1.17	1208	1.05	1179	1.07	736	7339
L-n2-wt20-I1	1514	1574	0.96	1494	1.01	1453	1.04	329	1835
L-n2-wt30-I1	1596	2009	0.79	1617	0.99	1538	1.04	194	815
L-n2-wt40-I1	1686	2416	0.70	1611	1.05	1488	1.13	110	459
L-n2-wt50-I1	1714	2543	0.67	1739	0.99	1585	1.08	92	294
L-n2-wt60-I1	1714	2633	0.65	1787	0.96	1600	1.07	71	204
L-n2-wt70-I1	1682	2660	0.63	1814	0.93	1597	1.05	55	150
L-n2-wt30-I0.5	1518	1868	0.81	1489	1.02	1410	1.08	171	815
L-n2-wt40-I0.5	1554	2326	0.67	1482	1.05	1361	1.14	95	459
L-n2-wt50-I0.5	1520	2450	0.62	1517	1.00	1364	1.11	67	294
L-n2-wt60-I0.5	1622	2537	0.64	1533	1.06	1352	1.20	49	204
L-n2-wt70-I0.5	1559	2487	0.63	1599	0.97	1393	1.12	42	150
L-n3-wt30-I2	1741	2478	0.70	1840	0.95	1692	1.03	110	815
L-n3-wt40-I2	1768	2166	0.82	1911	0.93	1713	1.03	75	459
L-n3-wt50-I2	1814	2174	0.83	1961	0.93	1720	1.05	55	294
L-n3-wt60-I2	1858	2168	0.86	1998	0.93	1721	1.08	43	204
L-n3-wt70-I2	1802	2125	0.85	2029	0.89	1718	1.05	34	150
L-n3-wt30-I1	1651	2260	0.73	1681	0.98	1542	1.07	101	815
L-n3-wt40-I1	1695	2139	0.79	1740	0.97	1555	1.09	67	459
L-n3-wt50-I1	1721	2153	0.80	1782	0.97	1557	1.11	49	294
L-n3-wt60-I1	1749	2150	0.81	1813	0.96	1554	1.13	37	204
L-n3-wt70-I1	1671	2111	0.79	1838	0.91	1549	1.08	29	150
L-n3-wt30-I0.5	1526	2042	0.75	1545	0.99	1413	1.08	91	815
L-n3-wt40-I0.5	1644	2112	0.78	1593	1.03	1419	1.16	59	459
L-n3-wt50-I0.5	1587	2131	0.74	1628	0.97	1417	1.12	42	294
L-n3-wt60-I0.5	1529	2132	0.72	1653	0.92	1411	1.08	31	204
L-n3-wt70-I0.5	1458	2096	0.70	1673	0.87	1405	1.04	24	150
L-n4-wt30-I2	1765	2650	0.67	1889	0.93	1682	1.05	68	815
L-n4-wt40-I2	1816	2003	0.91	1952	0.93	1693	1.07	46	459
L-n4-wt50-I2	1841	2005	0.92	1997	0.92	1694	1.09	34	294
L-n4-wt60-I2	1761	1990	0.88	2031	0.87	1690	1.04	26	204
L-n4-wt70-I2	1670	1937	0.86	2059	0.81	1685	0.99	21	150
L-n4-wt30-I1	1692	2395	0.71	1721	0.98	1531	1.11	62	815
L-n4-wt40-I1	1717	1997	0.86	1774	0.97	1536	1.12	42	459
L-n4-wt50-I1	1744	2002	0.87	1811	0.96	1532	1.14	30	294
L-n4-wt60-I1	1722	1989	0.87	1839	0.94	1526	1.13	23	204
L-n4-wt70-I1	1617	1939	0.83	1862	0.87	1519	1.06	18	150
L-n4-wt30-I0.5	1513	2146	0.71	1577	0.96	1401	1.08	56	815
L-n4-wt40-I0.5	1583	1989	0.80	1621	0.98	1400	1.13	37	459
L-n4-wt50-I0.5	1522	1998	0.76	1652	0.92	1394	1.09	26	294
L-n4-wt60-I0.5	1490	1987	0.75	1674	0.89	1385	1.08	20	204
L-n4-wt70-I0.5	1445	1939	0.75	1692	0.85	1377	1.05	15	150